Official Journal of the Society for Molecular Imaging

MOLECULAR IMAGING

Volume 4 · Number 1 · January – March 2005

Co-localizing DCE-MRI with Molecular Profiles in Prostate Cancer

3D Image Analysis of Fluorescent Drug Binding

An Imaging Agent for Dubin-Johnson Syndrome

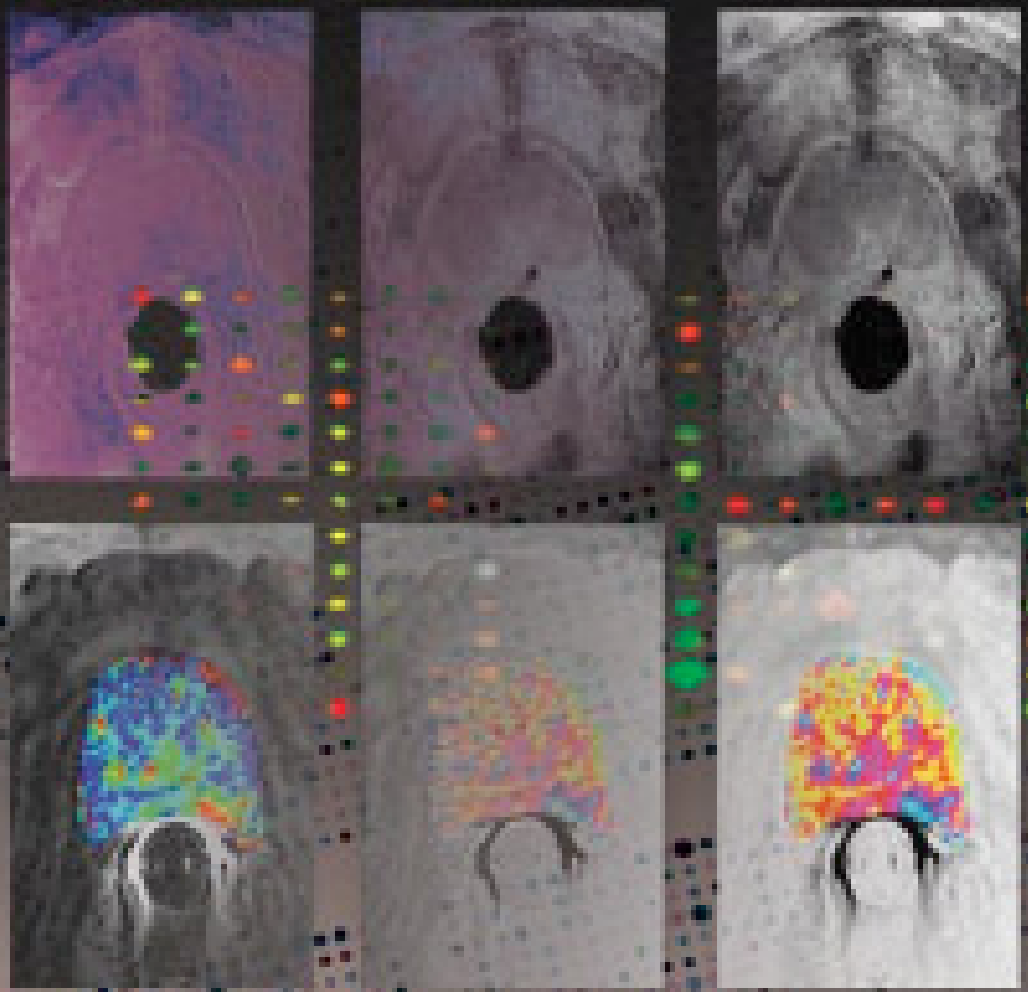

DECKER

Report Documentation Page

Form Approved
OMB No. 0704-0188

1. REPORT DATE	2. REPORT TYPE	3. DATES COVERED
OCT 2004		**00-00-2004 to 00-00-2004**

4. TITLE AND SUBTITLE	5a. CONTRACT NUMBER
An Interventional MRI Technique for the Molecular Characterization of Heterogeneous Intra-Prostatic Dynamic Contrast Enhancement	5b. GRANT NUMBER
	5c. PROGRAM ELEMENT NUMBER
6. AUTHOR(S)	5d. PROJECT NUMBER
	5e. TASK NUMBER
	5f. WORK UNIT NUMBER
7. PERFORMING ORGANIZATION NAME(S) AND ADDRESS(ES) **Johns Hopkins University School of Medicine,Department of Radiology,720 Rutland Avenue,Baltimore,MD,21205-2195**	8. PERFORMING ORGANIZATION REPORT NUMBER
9. SPONSORING/MONITORING AGENCY NAME(S) AND ADDRESS(ES)	10. SPONSOR/MONITOR'S ACRONYM(S)
	11. SPONSOR/MONITOR'S REPORT NUMBER(S)

12. DISTRIBUTION/AVAILABILITY STATEMENT
Approved for public release; distribution unlimited

13. SUPPLEMENTARY NOTES

14. ABSTRACT
see report

15. SUBJECT TERMS

16. SECURITY CLASSIFICATION OF:			17. LIMITATION OF ABSTRACT	18. NUMBER OF PAGES	19a. NAME OF RESPONSIBLE PERSON
a. REPORT **unclassified**	b. ABSTRACT **unclassified**	c. THIS PAGE **unclassified**	**Same as Report (SAR)**	**13**	

An Interventional MRI Technique for the Molecular Characterization of Heterogeneous Intra-Prostatic Dynamic Contrast Enhancement

Cynthia Ménard M.D. [1,2], Robert C. Susil Ph.D. [3], Peter Choyke M.D. [4], Jonathan Coleman MD[5], Robert Grubb M.D. [5] Ahmed Gharib M.D. [4] Axel Krieger M.S. [6] Peter Guion M.S.[1], David Thomasson Ph.D. [4] Karen Ullman R.T.T. [1], Sandeep Gupta [7] Virginia Espina M.S. [8]Lance Liotta M.D. [8] Emanuel Petricoin Ph.D. [9], Gabor Fitchtinger Ph.D. [6], Louis L. Whitcomb Ph.D. [6], Ergin Atalar Ph.D. [3], C. Norman Coleman M.D. [1], Kevin Camphausen M.D. [1]

[1]Radiation Oncology Branch, National Cancer Institute, NIH-DHHS
Bldg 10, Rm B3B69, 9000 Rockville Pike, Bethesda, MD, 20892

[2]Department of Radiation Oncology, Princess Margeret Hospital, University of Toronto, 610 University Ave, Toronto, ON, M5G 2M9, Canada

[3]Department of Biomedical Engineering, Johns Hopkins University School of Medicine, 720 Rutland Ave., Baltimore, Maryland, 21205

[4]Diagnostic Radiology Department, Clinical Center, NIH-DHHS
Bldg 10, Rm1C660, 9000 Rockville Pike, Bethesda, MD, 20892

[5]Urologic Oncology Branch, National Cancer Institute, NIH-DHHS
Bldg 10, Rm 2B47, 9000 Rockville Pike, Bethesda, MD, 20892

[6]Department of Mechanical Engineering, Johns Hopkins University School of Medicine, 123 Latrobe Hall, 3400 North Charles Street, Baltimore, MD, 21218-2681

[7]GE Medical Systems, USA

[8]FDA-NCI Clinical Proteomics Program, Laboratory of Pathology, Center for Cancer Research, National Cancer Institute, NIH-DHHS, Bldg 10, RmB1B53, 9000 Rockville Pike, Bethesda, MD, 20892

[9]FDA-NCI Clinical Proteomics Program, Office of Cellular and Gene Therapy Center for Biologics Evaluation and Research, Food and Drug Administration, 8800 Rockville Pike, Bldg 29A Room 2D12, Bethesda, MD, 20892

Submitted as a Brief Report to Molecular Imaging, October 13 2004

Corresponding author:
Cynthia Ménard
Department of Radiation Oncology, Princess Margaret Hospital
610 University Ave, Toronto, ON, M5G 2M9 Canada
Cynthia.Menard@rmp.uhn.on.ca
Phone: 416-946-2936 Fax: 416-946-2227

Key Words: angiogenesis, molecular imaging, interventional MRI, prostate cancer, microarray analysis

Sources of funding: Robert Susil was supported by an NIH MSTP fellowship. Supported in part by the following grants: NIH R01 EB002963, NSF EEC 9731478. U.S, Army Prostate Cancer Research Program Award DAMD17-01-1-0064, NSF ERC 9731478, and an NSF ERC PER grant.

Originality of the work: This work has not been previously published. It has been presented in part at the ISMRM annual meeting in Kyoto, Japan, May 2004, and at the Interventional MRI Symposium in Boston, MA October 2004.

Abstract

The biological characterization of an individual patient's tumor by non-invasive imaging will have an important role in cancer care and clinical research if the molecular processes that underlie the image data are known. Spatial heterogeneity in the dynamics of MRI contrast enhancement (DCE-MRI) is hypothesized to reflect variations in tumor angiogenesis. Here we demonstrate the feasibility of precisely co-localizing DCE-MRI data with the genomic and proteomic profiles of underlying biopsy tissue using a novel MRI-guided biopsy technique in a patient with prostate cancer.

Abbreviations:

DCE-MRI – Dynamic Contrast Enhanced Magnetic Resonance Imaging

GKM – General Kinetic Model

MR – Magnetic Resonance

MRI – Magnetic Resonance Imaging

ROI – Region of Interest

Introduction

Dynamic contrast-enhanced magnetic resonance imaging (DCE-MRI) provides a visual representation of both the anatomy and microvascular biology of cancer by measuring temporal changes in MR signal intensity associated with the intravascular injection of a contrast agent. (1) Spatial heterogeneity in the kinetics of contrast transit is thought to reflect variations in tissue perfusion and microvascular permeability.(2) Angiogenic microvessels, important for the growth and survival of cancer cells, are characterized in part by larger endothelial cell gaps resulting in greater permeability to small molecules.(3) Kinetic analysis of DCE-MRI is thus hypothesized to create an image reflecting the underlying malignant vasculature of an individual patient's tumor. There is mounting incentive to incorporate imaging surrogates, such as DCE-MRI, for patient selection and early measures of response in clinical trials of molecularly targeted anti-angiogenic therapies. (4) Imaging has the potential to provide more complete information on a tumor's microvascular biology, in contrast to information obtained from a biopsy, which may be subject to sampling error. In addition, imaging is non-invasive and spares the potential morbidities of biopsy, lending itself to serial measurements through a course of therapy.

However, data elucidating the molecular processes that underlie DCE-MRI and establishing its validity as a surrogate are lacking. Notable intraprostatic (5) and intratumoral (6) heterogeneity mandates millimeter co-localization accuracy between tissue samples and their corresponding image pixels. When prostate MR imaging and tissue acquisition procedures are performed in different settings and at different times, clinical co-registration is fraught with error. To address this key issue, we developed a technique for

MRI-guided needle biopsy of the prostate to be performed concurrently with a diagnostic MRI procedure inside a cylindrical 1.5T MRI scanner.

Methods

A patient with Stage I, intermediate-risk localized prostate cancer provided informed consent for enrollment on this IRB approved study. For the integrated procedure, the patient is positioned prone and a custom-designed interventional endorectal imaging coil is inserted and secured to the scanner table. A needle guide inside the stationary imaging coil contains MR tracking microcoils allowing for spatial registration of the device (R.C.S. et al, manuscript submitted, personal communication) (7). A continuous series of DCE-MR images of the prostate (3D spoiled GRE, scan time 5.1s, **Fig. IA**) are acquired before and during the injection of intravenous contrast (gadolinium chelate, 0.2mmol/kg, 3cc/s). The needle guide is translated and rotated within the endorectal coil until its trajectory, computed from the tracking coils, coincides with a biopsy target location defined on the diagnostic images. A 14G core biopsy needle is then inserted, its location is verified by MRI, and tissue is collected. **(Fig. IB and C)** This can be repeated for additional biopsy target sites within the prostate gland. The overall imaging and procedure time is approximately 90 minutes depending on the number of biopsies.

To analyze DCE-MRI data, a T1 map of the prostatic anatomy is first generated (8) to estimate the concentration of gadolinium chelate for a given signal intensity. Pixel data are submitted to a general kinetic model (GKM) fitting routine (9), which corrects the data for arterial input kinetics (measured over the external iliac artery) and implements a curve-

fitting solution to a GKM convolution integral. In this fashion, regions of interest (ROIs) encompassing those MR image pixels that correspond to the biopsy locations can be defined, and their corresponding time-intensity profiles and summary kinetic parameters computed. **(Fig. IE)** The transfer constant K^{trans} (corresponding to the magnitude of the enhancement curve, unit min^{-1}) and the rate constant k^{ep} (describing the rate of clearance, unit min^{-1}) are thought to reflect differences in tissue perfusion and microvascular permeability, respectively. The kinetic parameters are derived based on the following equation:

$$C_T(t) = K^{PS}\int C_P(\theta)e^{-k(t-\theta)}d\theta + f_{PV}C_P(t)$$

Where $C_T(t)$ = concentration of gadopentate in tumor tissue at any time t, K^{PS} = K_{TRANS}=endothelial transfer coefficient, C_P=concentration of gadopentate in the plasma space of the tumor tissue (assumed equal to that in the central venous blood plasma, i.e. input function), k= rate constant of reflux from interstitial water back to plasma, and $f_{PV=}$ fractional plasma volume of the tumor tissue.

To characterize the biological processes underlying the image data, needle biopsy specimens can be subjected to comprehensive histopathological, genomic, and proteomic analysis. Such analysis is chiefly enabled by microarray technology, which is distinguished by its comprehensive analytic capabilities using low sample volumes. In this case example, mRNA was isolated and amplified from snap frozen cores (10). The amplified mRNA was co-hybridized to a cDNA microarray with a reference standard. In turn, whole cell protein lysates from ethanol-fixed and paraffin-embedded tissue sections of

twin cores obtained at the same biopsy sites were analyzed using reverse phase protein arrays. (Ref 11 for detailed methods)

Early Results

We focused our initial analysis on signaling pathways known to be associated with angiogenesis. This case example shows differing levels of protein and gene expression at distinctive sites of contrast enhancement kinetics on DCE-MRI. **(Fig. 1I)** The level of hypoxia inducible factor (HIF-1α) mRNA and protein was lower at the site of higher contrast enhancement, while a number of other genes involved in angiogenesis signaling were upregulated. Some discordance observed at a single time point between protein and corresponding mRNA, for example AKT levels, supports the need for a comprehensive and serial analysis to evaluate mRNA/protein kinetics.

Conclusion

Our results show that the technical challenge of integrating needle-based prostate interventions with diagnostic MRI in a cylindrical clinical scanner can be overcome. Image subsites of interest can be precisely sampled, providing a research platform well suited to MRI and tissue correlation. The molecular profile prostate tissues underlying DCE-MRI will now be acquired in a larger series of patients in order to characterize the molecular biology of MR contrast enhancement. As we gain knowledge in the molecular biology underlying cancer and DCE-MRI, a more valid interpretation of an individual patients' tumor biology will ensue.

Acknowledgements: We thank A. Srikanchana for software support in DCE-MRI analysis, and Dr. M. Merino (Pathology).

References

1. Choyke PL, Dwyer AJ, Knopp MV (2003). Functional tumor imaging with dynamic contrast-enhanced magnetic resonance imaging. *J Magn Reson Imaging* 17:509-20.

2. Padhani AR, Dzik-Jurasz A (2004): Perfusion MR Imaging of Extracranial Tumor Angiogenesis. *Top Magn Reson Imaging* 15:41-57.

3. Dvorak HF, Nagy JA, Feng D, et al (1999). Vascular permeability factor/vascular endothelial growth factor and the significance of microvascular hyperpermeability in angiogenesis. *Curr Top Microbiol Immunol* 237:97-132.

4. Smith JJ, Sorensen AG, Thrall JH (2003). Biomarkers in imaging: realizing radiology's future. Radiology 227:633-8.

5. Aihara M, Wheeler TM, Ohori M, et al (1994). Heterogeneity of prostate cancer in radical prostatectomy specimens. *Urology* 43:60-6; discussion 66-7.

6. Evans SM, Hahn SM, Magarelli DP, et al (2001). Hypoxic heterogeneity in human tumors: EF5 binding, vasculature, necrosis, and proliferation. *Am J Clin Oncol* 24:467-72.

7. Krieger A, Susil RC, Ménard C, et al (2004). Design of a Novel MRI Compatible Manipulator for Image Guided Prostate Interventions. *IEEE Transactions on Biomedical Engineering*, In press.

8. Deoni SC, Rutt BK, Peters TM (2003). Rapid combined T1 and T2 mapping using gradient recalled acquisition in the steady state. *Magn Reson Med* 49:515-26.

9. Kety S (1960): Blood Tissue Exchange Methods; Theory of Blood Tissue Exchange and it's Application to Measurement of Blood Flow. *Meth. Med. Res*. 8:223-227.

10. Goley EM, Anderson S, Ménard C, et al (2004). Microarray analysis in clinical oncology: pre-clinical optimization using needle core biopsies from xenograft tumors. *BMC Cancer* 4:20.

11. Espina V, Mehta AI, Winters ME, et al (2003): Protein microarrays: molecular profiling technologies for clinical specimens. Proteomics 3:2091-100.

Figure Legends

Figure I: Prostate interventional MRI for the correlation of molecular biology and DCE-MRI. The stationary interventional endorectal coil **(∗)** is used for both diagnostic and interventional MR imaging. **(a)** DCE-MRI at 120s shows a small area of increased signal intensity in the left peripheral zone of the prostate. ROIs (red an blue) corresponding to the subsequent needle biopsy voids **(b,c)** are defined for image analysis. **(e)** Time-intensity curves (corrected for T1 heterogeneity) from each ROI are fit to a GKM convolution integral using an arterial input function measured from the external iliac artery. The transfer constant K^{trans} (corresponding to the magnitude of the enhancement curve, unit min^{-1}) and the rate constant k^{ep} (describing the rate of clearance, unit min^{-1}) are thought to reflect differences in the perfusion and microvascular permeability underlying each ROI, respectively.[2] H&E staining shows adenocarcinoma **(d)** corresponding to higher K^{trans} and k^{ep} than benign tissue **(f)**. cDNA microarray **(g,k)** and reverse phase protein array **(h,j-**array probed with STAT3 antibody shown**)** (11) results show differing trends of protein and gene expression levels **(i)** from benign (blue ROI) to malignant (red ROI) tissue obtained at distinctive sites of contrast enhancement kinetics on DCE-MRI.

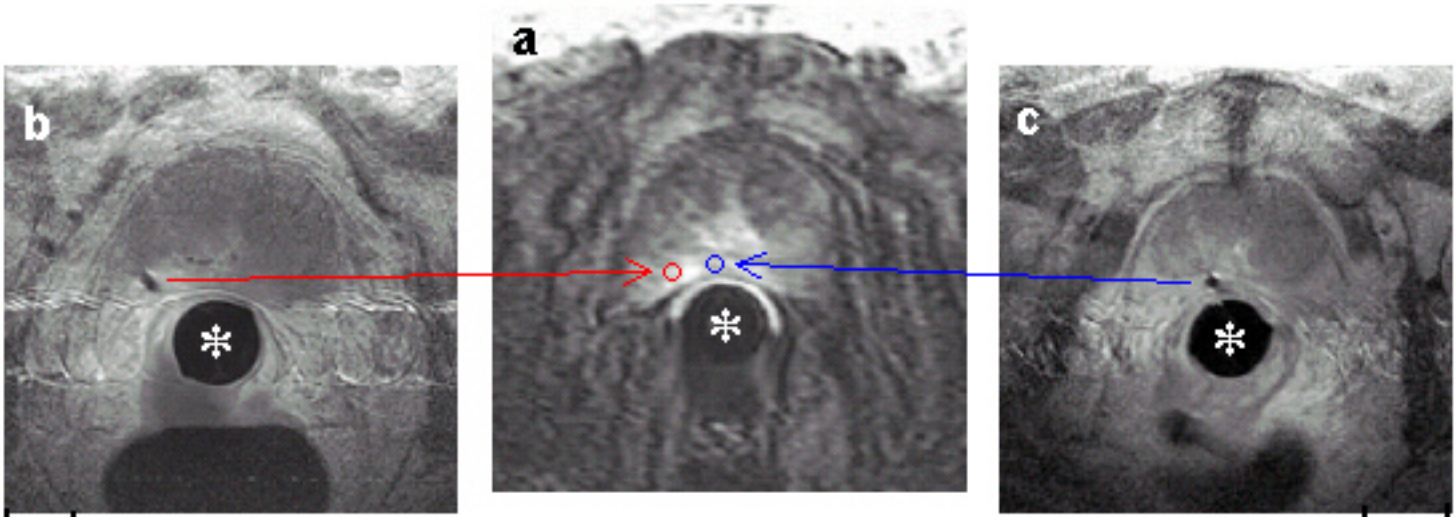

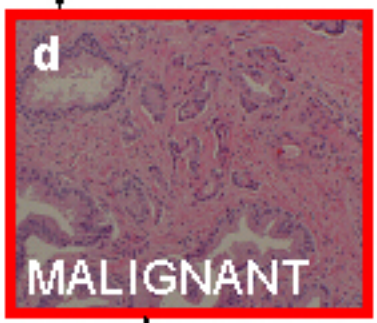

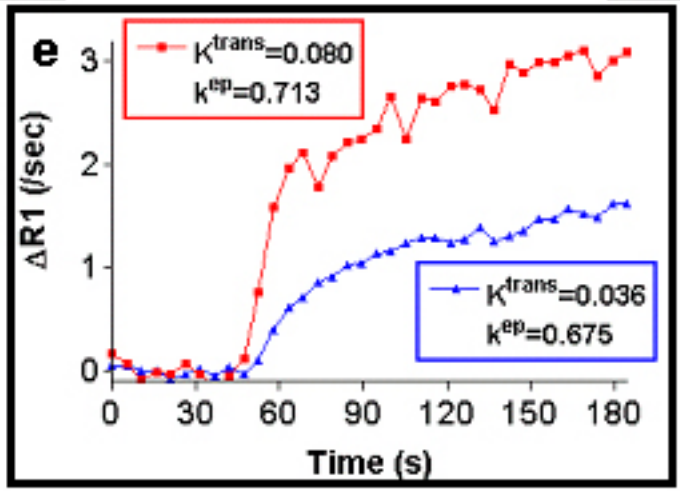

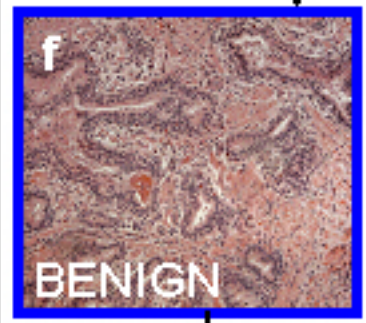

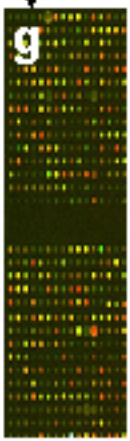

i

Array	Pathway	↑	↓
cDNA Microarray	Hypoxia	NOS3, VHL	HIF1A
	PDGF	MAPK8, STAT3 PDGFRA	FOS, JUN, MAP2K1&4
	AKT	AKT1	EIF2S1&3
Protein Array	Hypoxia	-	HIF1a, eNOS
	PDGF	-	PDGFβ, pPDGFβ, STAT3
	AKT	-	AKT, pAKT, EIF4G